Enhancement of the corrosion resistance for stainless steel 316 by applying laser shock peening

Sarah A. Jasim[1], Ammar Ayesh[2], A. Kadhim[3], Oday I. Abdullah[4, 5, 6*]

[1]College of Science, Diyala University, Iraq, Email: sarahmaster91@gmail.com
[2]Physics Dept.College of Science, Diyala University, Iraq, Email: ammarayesh@uodiyala.edu.iq
[3]Laser and Optoelectronic Eng. Dept., University of Technology, Iraq, Email: abdulhadi.k.judran@uotechnology.edu.iq
[4]Department of Energy Engineering, College of Engineering, University of Baghdad, Iraq
[5]Mechanical Engineering Department, College of Engineering, Gulf University, Sanad 26489, Bahrain
[6]Department of Mechanics, Al-Farabi Kazakh National University, Almaty 050040, Kazakhstan
*Corresponding author: e-mail: oday.abdullah@tuhh.de

This research paper focuses on enhancing the surface characteristics of the 316 stainless steel (SS316) alloy, including roughness, microhardness, and corrosion resistance. Where the application of ND-YAG laser technology, a highly relevant and timely area, was investigated deeply. The Q-switching Nd: YAG Laser was used with varying laser energy levels within the context of the laser shock peening (LSP) technique. The corrosion resistance of the 316 ss alloy is evaluated in a corrosive environment of 500 mL of saliva (with a pH of 5.6) through electrochemical corrosion testing. Corrosion rate was determined based on the analysis of polarization curves. The outcomes of this research reveal that as the laser energy was increased, there was a noticeable enhancement in the mechanical properties of the 316 ss alloy's surface. Importantly, the corrosion rate experiences a significant reduction, decreasing from 4.94 mm/yr to 3.59 mm/yr following laser shock peening (LSP) application.

Keywords: ND-YAG laser, corrosion, 316 ss Alloy, saliva.

INTRODUCTION

Corrosion, in the context of materials science, is characterized by the deterioration of metals and their alloys from chemical or electrochemical interactions with the surrounding environment[1]. The corrosion reactions are classified based on the type of corrosive environments (wet and dry corrosion)[2, 3]. Furthermore, corrosion can manifest in different forms based on the morphology of the damage inflicted upon the metal. This includes general corrosion, crevice corrosion, pitting corrosion, intergranular corrosion, de-alloying, environmentally induced fracture, erosion-corrosion, and galvanic corrosion[4]. Various methods have been used to protect metals from corrosion, such as alloying, coating, cathodic protection, and anodic protection. Recently, laser technology has emerged as a promising approach for enhancing metal properties, including surface roughness, hardness, and corrosion resistance[5]. Additionally, the application of corrosion inhibitors holds practical significance, as they play a vital role in reducing metallic waste and mitigating the risk of material loss, which disrupt industrial processes and incurs additional costs[6].

Laser technology has gained prominence in material processing, offering unique advantages over traditional energy sources. These advantages include automation capabilities, high productivity, non-contact processing, reduced processing costs, elimination of finishing operations, optimized material utilization, and improved product quality[7]. One specific application of laser technology is laser peening, a cold working process that enhances the surface of metals by introducing compressive residual stresses. These compressive stresses are instrumental in preventing surface deterioration effects by impeding crack initiation. Laser peening offers control and the ability to access hard-to-reach areas of components, making it suitable for both new and in-service parts[8].

The benefits of laser peening translate into increased service life, extended maintenance intervals, and reduced downtime–all without necessitating changes to the part's original design. Industries such as aerospace, power generation, automotive, maritime, heavy equipment, and manufacturing have embraced laser peening to optimize the performance of lightweight components while maintaining or improving metal fatigue strength[8, 9]. In the realm of corrosion, the categorization of reactions based on the corrosive environment's characteristics distinguishes between wet and dry corrosion[9, 10]. Stainless steel 316 L is an austenitic steel used in chemical industries, oil and gas industries, biomedical applications, pressure vessels, boilers, heat exchangers, etc., for its excellent corrosion resistance properties. The corrosion resistance is due to the formation of passive chromium oxide film. The corrosion resistance is uncompromised in the aqueous and aerated environment. This research focuses on enhancing the surface characteristics of the 316 stainless steel (316 ss) alloy, including roughness, microhardness, and corrosion resistance. The research focuses on the application of ND-YAG laser technology, a highly relevant and timely area of investigation. The material of interest in this study is the 316 ss alloy. The Q-switching Nd: YAG Laser was used with varying laser energy levels, within the context of the laser shock peening (LSP) technique.

EXPERIMENTAL METHODS

Q-switching Nd-YaG laser

Figure 1 illustrates the experimental setup used in this study, featuring a Q-switch Nd-YaG laser with different parameters, as mentioned in Table 1. The material under investigation is 316 stainless steel (316 ss), cut into circular pieces with a diameter of 20 mm and thickness of 5 mm. These samples are subsequently immersed in double-distilled deionized water (DDDW). In the surface treatment process, the laser pulse is directed onto the surface of 316 ss. As the laser pulse traverses the

confinement layer, it makes contact with the sample, resulting in the formation of plasma. This expanding plasma plume exerts high pressure on the surface of the sample, a technique commonly referred to as Laser Shock Peening.

Table 1. Laser shock peening parameters

Material	316 stainless steel A
Laser wavelength	1064 nm
Repetition rate	3 Hz
Pulse duration	10 ns
Energy	200–1000 MJ
Number of pulses	1250 pulse
Laser spot size	1.2 mm
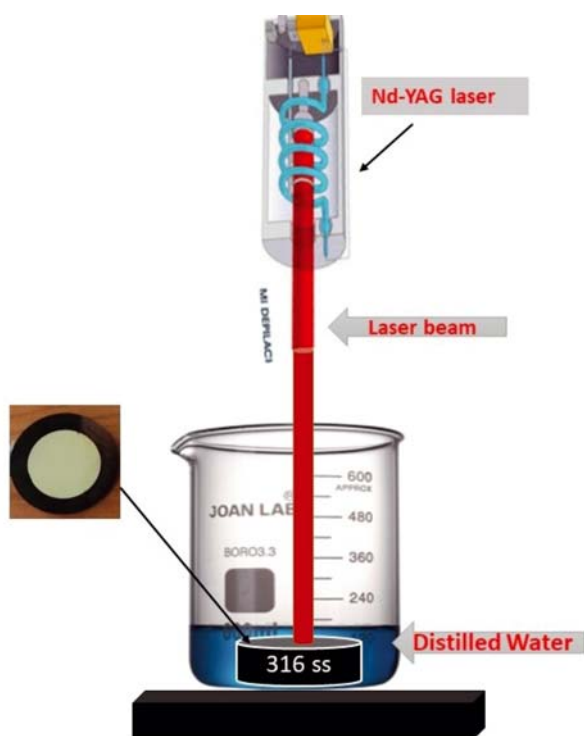
Figure 1. Laser shock peening technique

Samples Preparation

The sample preparation procedure involved cutting them into round pieces with a 20 mm diameter and a 5 mm thickness with the help of a turning machine. Afterward, the samples were meticulously cleaned by washing them with distilled water and methanol. Following this, they were carefully dried and shielded from exposure to ambient air. In order to achieve a uniform surface texture and roughness for evaluation purposes, the samples underwent a grinding process using different metallographic papers such as SiC and AlC. Furthermore, an additional refinement step was carried out using polishing paper coated with Al_2O_3. This surface polishing process was completed using a processor polisher machine of the type Mopao 160 E. Subsequently, a thorough cleaning was performed using de-ionized water and ethanol to eliminate impurities and prevent metal oxidation. An epoxy material (A:B) was employed to securely mount the samples, with a mixing ratio of 2:1. This mounting process consists of placing the samples in a metal mold and allowing them to harden for approximately fifteen minutes. Following the mounting process, external wires were attached to the samples to ensure accessibility when they were placed in the corrosion cells. Additionally, the connection between the sample and the wire was verified using an ohmmeter device before initiating the corrosion procedure.
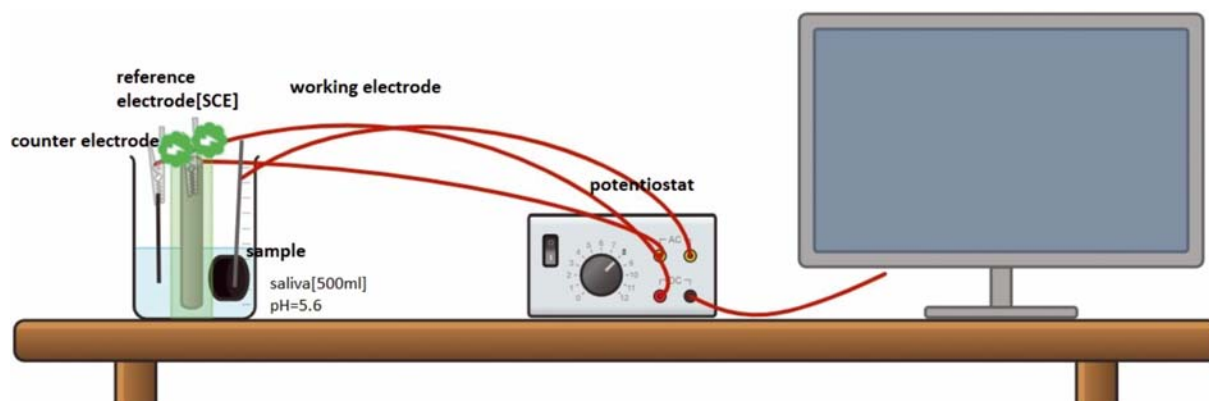
Corrosion test

Voltammetric measurements were measured using a potentiostat/galvanostat (DY2323, manufactured by Digi-ivy, Inc.), as shown in Figure 2. The evaluation of corrosion resistance for the deposits was performed in a saliva solution with a pH of 5.6, serving as the corrosive medium at room temperature and without agitation. The electrochemical cell was composed of three electrodes: (i) An Ag/AgCl electrode as the reference electrode, (ii) platinum (Pt) as the counter electrode, and (iii) The 316 ss as the working electrode[10]. In order to prevent surface corrosion, the samples were protected with adhesive polymer, ensuring that only 1.0 cm^2 of the surface was in contact with the electrolyte. Linear sweep voltammetry (LSV) was recorded within a potential range of ±4000 mV at a scan rate of 0.1 V/s. The data was collected using the Corr Tests software package, which enabled the calculation of corrosion parameters such as corrosion current density (icorr) and polarization resistance (Rp) through the Tafel slope method[10, 11].

RESULTS AND DISCUSSIONS

Chemical Compositions

The chemical composition of the samples utilized in this study was determined using SPECTRO MAXx Instruments from AMETEK materials analysis. Detailed information is provided in Table 2.


Figure 2. The parts of the corrosion test rig

Table 2. Chemical composition of 316 stainless steel

| Compositions	C	Cr	Ni	Mn	Mo	Si	P	S	N	Co	Fe
wt%	0.049	16.817	10.02	1.109	2.093	0.454	0.029	0.001	0.005	0.205	Base

Microhardness result

The Vickers hardness method was used to assess the micro-hardness of samples before and after the laser treatment. The laser shock processing (LSP) was conducted under consistent conditions, including a fixed laser energy ranging from 200 to 1000 MJ and a DDDW of 30 mm. Before LSP, the alloys' average micro-hardness value stood at approximately 230.7 HV. Following the LSP treatment, the measurements exhibited variations, ranging from 225.9 HV (at a pulse energy of 200 MJ) to 325.2 HV (at a pulse energy of 1000 MJ) for 316 ss, as illustrated in Figure 3. The laser shock processing pulse energy escalation resulted in more pronounced grain refinement. Consequently, after LSP, the microhardness of the surface increased primarily due to the effects of dislocation strengthening and grain refinement. This observed behavior aligns with the findings in reference[12].
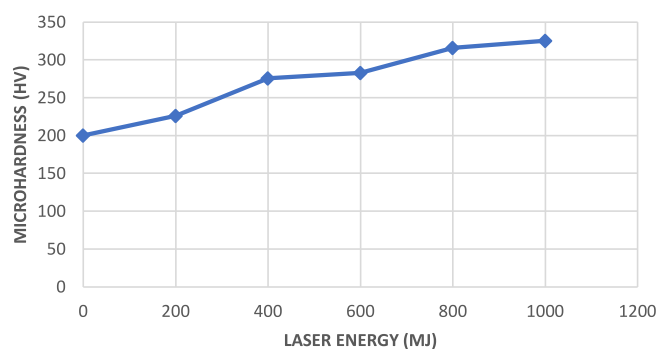
Figure 3. The variation of microhardness with the applied laser energy

Surface Roughness

Surface roughness measurements were conducted on all samples both before and after laser shock peening (LSP) treatment. The initial average surface roughness value prior to LSP processing for the samples was recorded as Ra = 0.03 nm. Post-LSP, the surface roughness values exhibited an increase, reaching Ra = 0.18 nm at an energy level of 1000 MJ, as depicted in Figure 4. This phenomenon can be attributed to the ablation processes associated with the interaction of the laser shock wave with the sample's surface. Consequently, an escalation in laser pulse energy corresponds to an increase in surface roughness, aligning with the findings in reference[13].
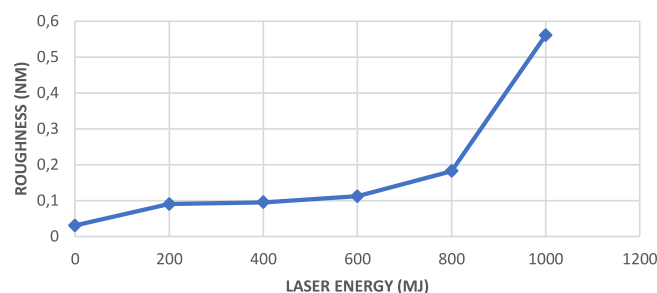
Figure 4. The variation of surface roughness with the laser energy

Microstructure Results

In this section, it will present the results of the Microstructure. Figure 5 depicts an alloy's surface microstructure after Laser Shock Peening (LSP). As laser shock waves interact with both the alloy and itself, their kinetic energy is converted into plastic deformation energy. It rapidly increases dislocation concentration, deformation twin formation, and stacking fault formation – hallmark features of plastic deformation in austenitic stainless steels[14].

Disturbances contribute significantly to hardening effects, while twin boundaries impose dislocation slip, as reference[15] explained. Hardening reaches its pinnacle on surfaces where LSP-induced plastic deformation has reached its maximum levels. Also, it's worth mentioning that the plastic deformation increases gradually with increasing laser energy levels.

Microstructures composed of dislocations, stacking faults, and deformation twins serve as convincing evidence of alloy resilience. When applied to 316 stainless steel
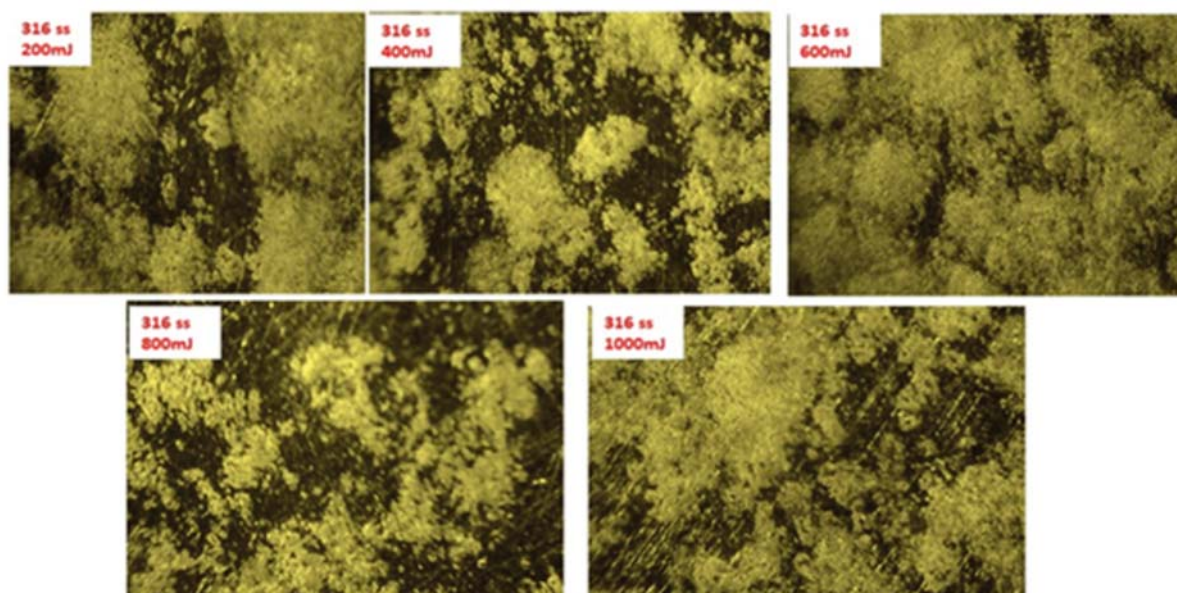
Figure 5. Microstructure of the sample after LSP for SS316 alloys applying different laser energy

(316 ss) alloys specifically, 1250 laser pulses at various energy levels produce comprehensive surface coverage. Their visual representation evokes images resembling sponge-like structures with nano and microporous layers that resemble sponges.

Corrosion resistance results

The impact of Nd: YAG laser energy on corrosion resistance was investigated across various laser energy levels, ranging from 200 to 1000 MJ as shown in Table 3, immersed in saliva at pH = 5.6 for studying the cor-

Table 3. LSP conditions

LSP conditions	The values
Laser wavelength	1064 nm
Laser energy	(0,200,400,600,800,1000)MJ
No. of pulses	1250
Pulse repetition rate	10 Hz
Confinement layer thickness	3 mm
Spot size	1.5 mm

rosion behavior. The corrosion rate results were found according to different laser energies, and what can be noticed through these results is that the minimum value of corrosion current (Icorr.) and corrosion potential (Ecorr.) are 34.627 $\mu A/cm^2$ and 550.75 mV, respectively at the energy of laser = 1000 MJ. The corresponding experimental measurements are detailed in Table 4. Figures 6–11 present the Tafel plots for 316 alloys, revealing a noticeable reduction in corrosion rates. These findings serve as an indicator of LSP's impact on corrosion rate reduction. The observed reduction in corrosion rates can be attributed to the heightened pressure generated by the shock wave during laser ablation, coupled with the increased surface exposure to laser pulses. This increases the surface hardness and irregularity of the samples, enhancing their corrosion resistance. These trends align with findings from prior research[16, 17]. Figures 6–11 depict the relationship between laser energy and corrosion rate graphically. In addition, Figure 12
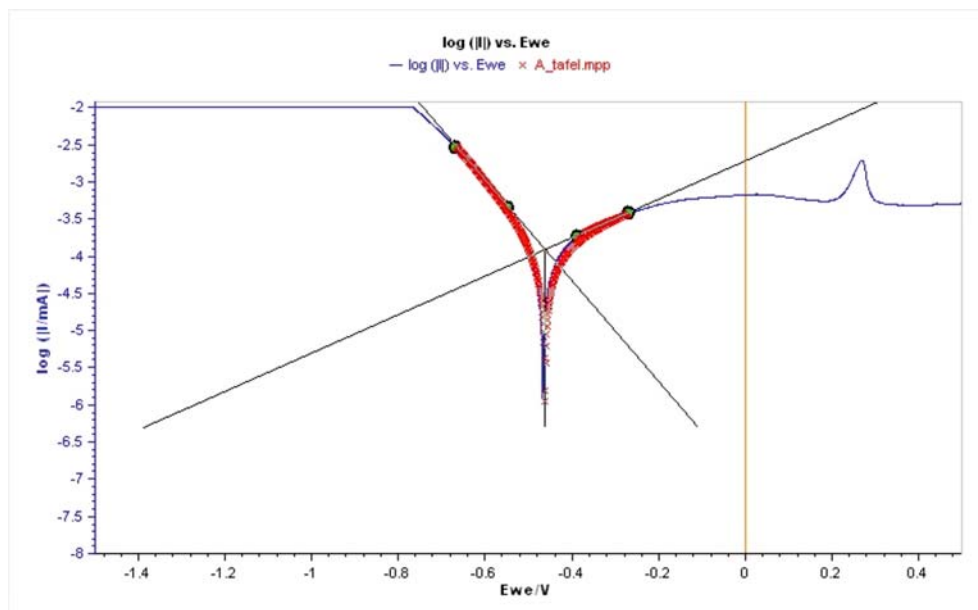
Figure 6. Tafel plot of 316 SS alloy before LSP
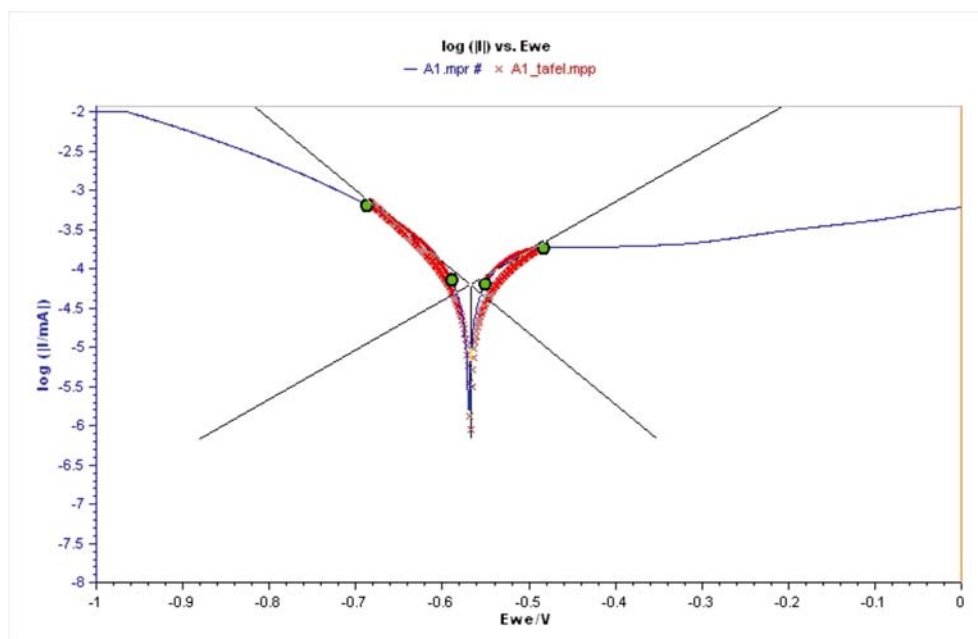
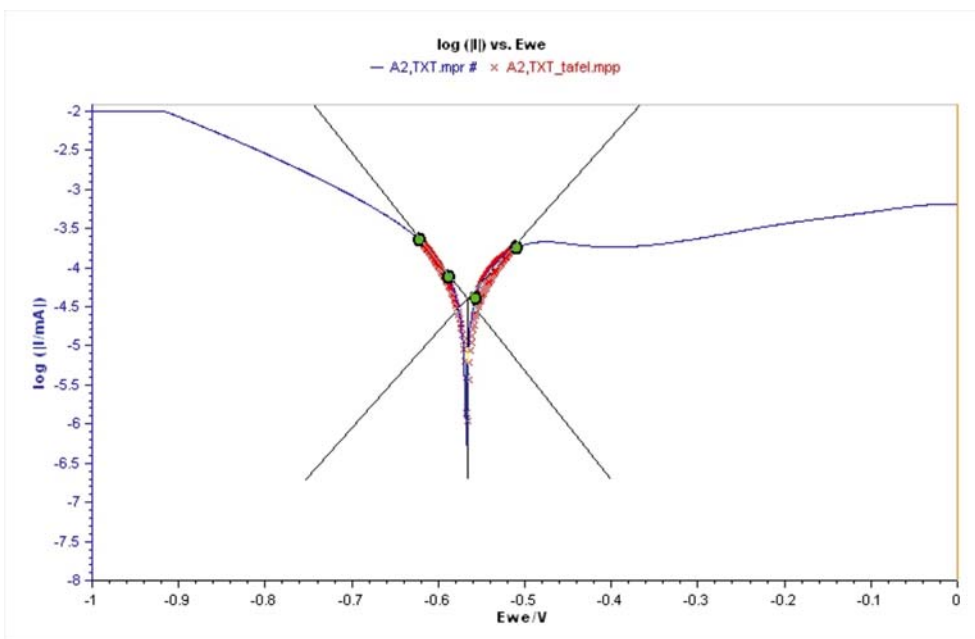**Figure 7.** Tafel plot of 316 SS alloy at energy 200 MJ

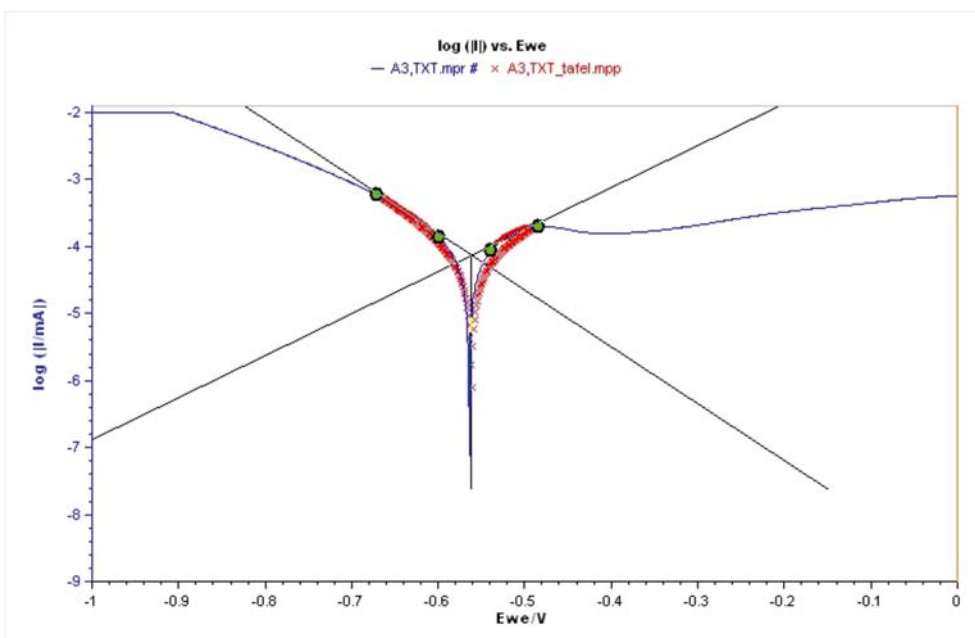**Figure 8.** Tafel plot of 316 SS alloy at energy 400 MJ

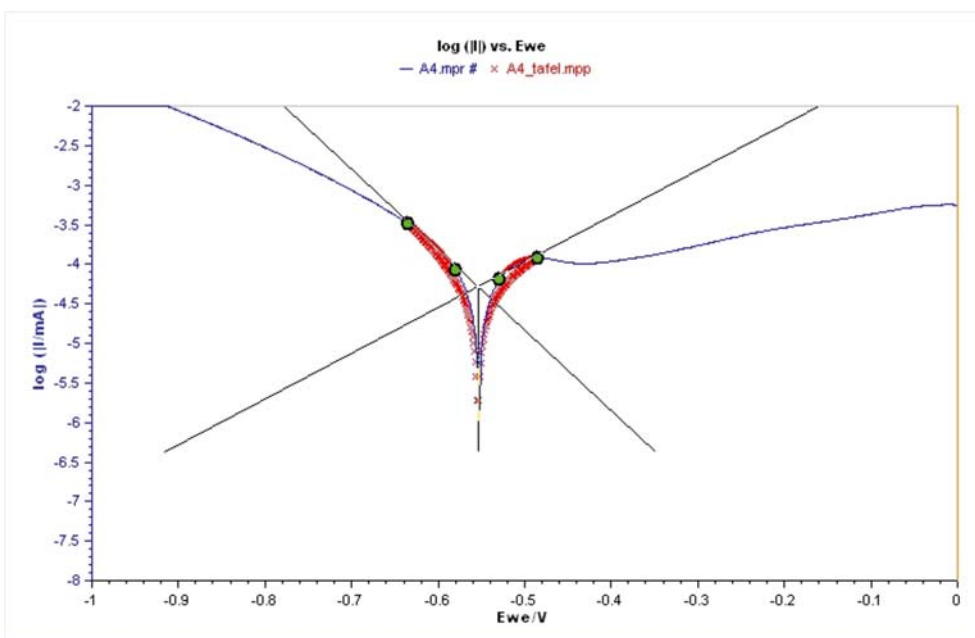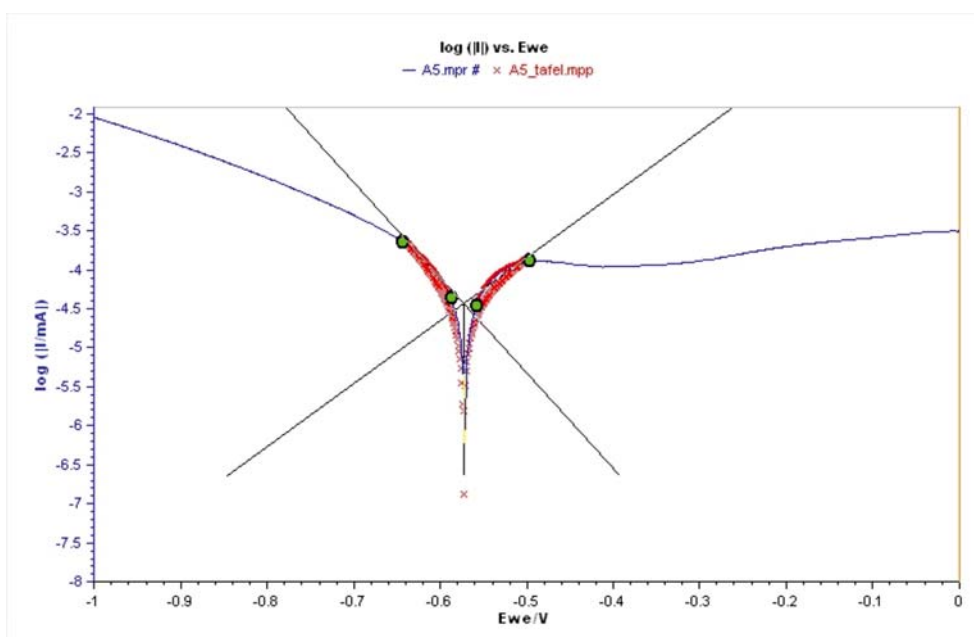**Figure 9.** Tafel plot of 316 SS alloy at energy 600 MJ

Figure 10. Tafel plot of 316 SS alloy at energy 800 MJ

Table 4. Polarization measurement at different laser energies for 316 alloy under artificial saliva of PH = 5.6

Laser energy(MJ)	icorr (µA/cm2)	Ecorr (mV)	ba (mV/dec)	bc (mV/dec)	Rp (kΩ.cm2)
0	188.959	–469.39	400.8	135.8	1.889
200	67.854	–560.07	123.1	122.0	0.678
400	53.329	–573.03	144.2	89.0	0.533
600	37.699	–564.46	78.6	64.1	0.376
800	37.409	–568.13	116.8	95.7	0.374
1000	34.627	–550.75	86.5	77.8	0.346

Table 5. The measurement at different laser energies for SS316 alloy under artificial saliva of PH = 5.6

Laser energy (MJ)	Microhardness (HV)	Roughness (nm)	Corrosion rate (mm/y)	Efficiency %
0	200	0.03	4.94	0
200	225.9	0.09	4.58	67
400	275.4	0.095	4.85	71
600	282.6	0.112	4.32	80
800	315.7	0.182	3.926	80.2
1000	325.2	0.56	3.59	81

Figure 11. Tafel plot of 316 SS alloy at energy 1000 MJ
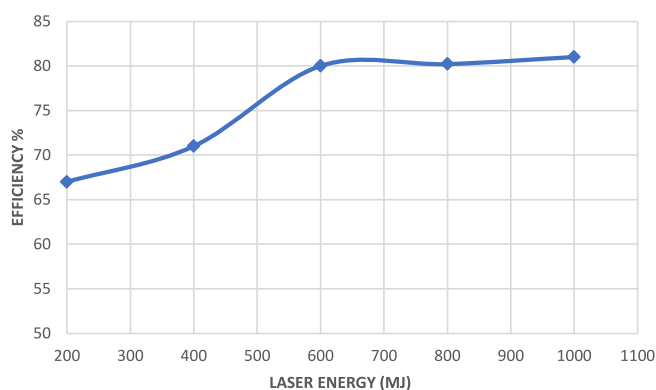
Figure 12. The variation of inhibition efficiency with laser energy for SS316

illustrates the corrosion-inhibiting effectiveness attained by LSP processing in a saliva medium. The corrosion rate decreased from 4.49 to 3.59 mm/yr, and the efficiency of the inhibitor increased from 67 to 81% with a rise in laser energy, as shown in 12. More details about the final results of the measurements can be seen in Table 5.

CONCLUSIONS AND REMARKS

Laser shock peening is an effective surface modification technique, yielding notable improvements in corrosion resistance. Post-LSP treatment, the corrosion rate exhibits a significant reduction, decreasing from 4.940 mm/y to 3.590 mm/y, with variations observed at different laser energy levels. Simultaneously, increasing laser energies gradually enhanced the mechanical properties like surface roughness and microhardness. The amplified surface exposure to laser pulses contributes to heightened surface hardness and roughness, subsequently influencing the corrosion rate in a live environment. Consequently, this results in an overall improvement in corrosion resistance for the utilized alloy. Ultimately, it can be noticed that the corrosion efficiency gradually increased, corresponding to the laser energy employed. Q-switching Nd: YAG laser is an efficient corrosion inhibitor for 316 ss alloy that is immersed in saliva. The higher inhibitor efficiency is 81%. In the future, investigations will use another inhibitor, like coating the alloy with nanoparticles that increase the corrosion resistance.

University of Technology for their invaluable guidance and support in achieving this research.

LITERATURE CITED

1. Wang, Y., Wang, W., Liu, Y., Zhong, L. & Wang, J. (2011). Study of localized corrosion of 304 stainless steel under chloride solution droplets using the wire beam electrode. *J. Corros. Sci.*, 53(9), 2963–2968. DOI: 10.1016/j.corsci.2011.05.051.

2. Koushik, B.G., Van den Steen, N., Mamme, M.H., Van Ingelgem, Y. & Terryn, H. (2021). Review on modelling of corrosion under droplet electrolyte for predicting atmospheric corrosion rate. *J. Mater. Sci. Technol.* 62, 254–267. DOI: 10.1016/j.jmst.2020.04.061.

3. Guo, M., Tang, J., Peng, C., Li, X., Wang, C., Pan, C. & Wang, Z. (2022). Effects of salts and its mixing ratio on the corrosion behavior of 316 stainless steel exposed to a simulated salt-lake atmospheric environment. *Mater. Chem. Phys.* 276, 125380. DOI: 10.1016/j.matchemphys.2021.125380.

4. Grum, J. (2007). Comparison of Different Techniques of Laser Surface Hardening. *J. Achiev. in Mater. Manufac. Engin.* 24(1), 17–25.

5. Xiong, Y., He, T., Guo, Z., He, H., Ren, F. & Volinsky, A.A. (2013). Effects of laser shock processing on surface microstructure and mechanical properties of ultrafine-grained high carbon steel. *Mater. Sci. Engin: A*, 570, 82–86. DOI: 10.1016/j.msea.2013.01.068.

6. Judran, A.K., Kadhim, S.M. & Elah, H.A. (2018). Enhancement of the corrosion resistance for 6009 aluminum alloy by laser treatment. *Kufa J. Eng.* 9, 201–214. DOI: 10.30572/2018/kje/090215.

7. Maaß, P. & Peißker, P. (2011). *Handbook of hot-dip galvanization* (13 Volume). John Wiley & Sons.(Eds.), Corrossion Handbook.

8. Khalil, K.S. (2014). Corrosion Inhibition Measurement of Zinc in Acidic Media by Different Techniques. Unpublished M.Sc. Thesis, University of Baghdad, Baghdad, Iraq.

9. Davis, J.R. (Ed.). (2001). *Surface Engineering For Corrosion And Wear Resistance* (1st Ed). USA, ASM international.

10. Akchurin, A., Bosman, R., Lugt, P.M. & van Drogen, M. (2016). Analysis of wear particles formed in boundary-lubricated sliding contacts. Tribology letters, 63, 1–14. DOI: 10.1007/s11249-016-0701-z.

11. Zhang, L., Zhang, Y.K., Lu, J.Z., Dai, F.Z., Feng, A.X., Luo, K.Y., J.S. Zhong, Q.W., Wang, M. & Qi, H. (2013). Effects of laser shock processing on electrochemical corrosion resistance of ANSI 304 stainless steel weldments after cavitation erosion. *J. Corros. Sci.* 66, 5–13. DOI: 10.1016/j.corsci.2012.08.034.

12. Sakthivel, N. (2018). *Analysis of Wear and Corrosion Properties of 316 L Stainless Steel Additively Manufactured Using Laser Engineered Net Shaping*, Doctoral Dissertation, Oklahoma State University, USA.

13. Yan, X., Wang, F., Deng, L., Zhang, C., Lu, Y., Nastasi, M., & Cui, B. (2018). Effect of laser shock peening on the microstructures and properties of oxide-dispersion-strengthened austenitic steels. *Adv. Engin. Mater.* 20(3), 1700641. DOI: 10.1002/adem.201700641.

14. Pan, X., Gu, Z., Qiu, H., Feng, A. & Li, J. (2022). Study of the mechanical properties and microstructural response with laser shock peening on 40CrMo steel. Metals, 12(6), 1034.

15. Lu, J., Qi, H., Luo, K., Luo, M. & Cheng, X. (2014)."Corrosion behaviour of AISI 304 stainless steel subjected to massive laser shock peening impacts with different pulse energies," *Corros. Sci.* 80, 53–59. DOI: 10.3390/met12061034.

16. Liu, D., Shi, Y., Liu, J. & Wen, L. (2019). Effect of laser shock peening on corrosion resistance of 316L stainless steel laser welded joint. *J. Surf. Coat. Technol.* 378, 124824. DOI: 10.1016/j.surfcoat.2019.07.048.

17. Guan, L., Ye, Z.X., Yang, X.Y., Cai, J.M., Li, Y., Li, Y. & Wang, G. (2021). Pitting resistance of 316 stainless steel after laser shock peening: Determinants of microstructural and mechanical modifications. *J. Mater. Proces. Technol.* 294, 117091. DOI: 10.1016/j.jmatprotec.2021.117091.